



Published in final edited form as:

*Nanomedicine*. 2018 October ; 14(7): 2465–2474. doi:10.1016/j.nano.2017.02.022.

## Gradient Nanocomposite Hydrogels for Interface Tissue Engineering

Lauren M. Cross<sup>a</sup>, Kunal Shah<sup>a</sup>, Sowmiya Palani<sup>a</sup>, Charles W. Peak<sup>a</sup>, and Akhilesh K. Gaharwar<sup>a,b,c,\*</sup>

<sup>a</sup>Department of Biomedical Engineering, Texas A&M University, College Station, TX 77841, USA

<sup>b</sup>Department of Materials Science and Engineering, Texas A&M University, College Station, TX 778413, USA

<sup>c</sup>Center for Remote Health Technologies and Systems, Texas A&M University, College Station, TX 77843, USA

### Abstract

Two-dimensional (2D) nanomaterials are emerging class of materials with unique physical and chemical properties due to high surface area and disc-like shape. Recently, these 2D nanomaterials are investigated for a range of biomedical applications including tissue engineering, therapeutic delivery and bioimaging, due to their ability to physically reinforce polymeric networks. Here, we present a facile fabrication of a gradient scaffold with two natural polymers (gelatin methacryloyl (GelMA) and methacrylated kappa carrageenan (MkCA)) reinforced with 2D nanosilicates to mimic the native tissue interface. The addition of nanosilicates results in shear-thinning characteristics of prepolymer solution and increases the mechanical stiffness of crosslinked gradient structure. A gradient in mechanical properties, microstructures and cell adhesion characteristics was obtained using a microengineered flow channel. The gradient structure can be used to understand cell-matrix interactions and to design gradient scaffolds for mimicking tissue interfaces.

### Graphical Abstract

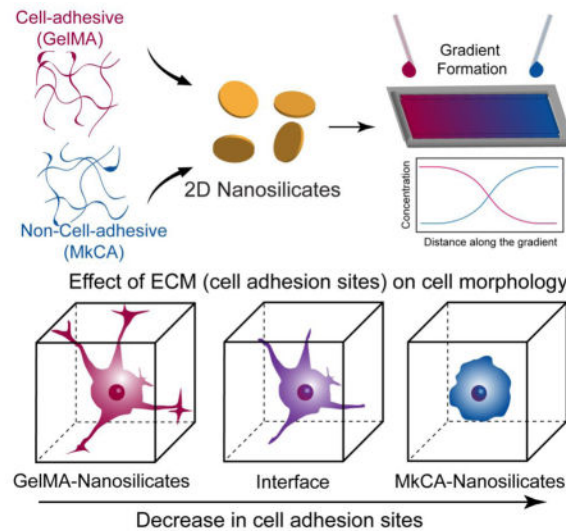
We present a facile fabrication of a gradient scaffold with two natural polymers (gelatin methacrylate (GelMA) and methacrylated kappa carrageenan (MkCA)) reinforced with 2D nanosilicates to mimic the native tissue interface. A gradient in mechanical properties, microstructures and cell adhesion characteristics was achieved. This simple approach could be applied to regeneration of tissue interfaces where a natural gradient in the structural, mechanical, and biological properties exists.

---

\*Corresponding author: gaharwar@tamu.edu (AKG).

Conflicts of interest: None

**Publisher's Disclaimer:** This is a PDF file of an unedited manuscript that has been accepted for publication. As a service to our customers we are providing this early version of the manuscript. The manuscript will undergo copyediting, typesetting, and review of the resulting proof before it is published in its final citable form. Please note that during the production process errors may be discovered which could affect the content, and all legal disclaimers that apply to the journal pertain.



## Keywords

Two-dimensional (2D) nanomaterials; Tissue engineering; Hydrogels; Gradient structure; Nanocomposites

## INTRODUCTION

The bone-cartilage interface is composed of cartilage and subchondral bone, with a gradient in structural, physical and chemical properties.<sup>1, 2</sup> For diseases such as osteoarthritis, it is difficult to engineer these complex architectures using conventional fabrication technologies to facilitate regeneration of damaged tissues. The ability to mimic such interfaces, as well as to control the cell-matrix interactions at different locations, will be needed to develop new approaches. A range of designs such as layered or gradient structures are developed to mimic gradient in structure and mechanical properties.<sup>3, 4</sup> Additionally, the native tissue interface is composed of both micro- and nanostructures, making nanoengineered biomaterials an ideal scaffold material to mimic the native architecture.<sup>5</sup> A range of nanomaterials are incorporated within polymeric networks to improve the structural, mechanical, or biological properties of the scaffold. For example, spherical nanoparticles such as hydroxyapatite, iron oxide, silica, have been extensively investigated to mimic the bone-cartilage interface, as it enhances cell proliferation and scaffold mechanical properties.<sup>6–12</sup>

Two dimensional (2D) nanomaterials have become a major focus in materials research in many applications, including biomedicine.<sup>13–15</sup> Importantly, they possess the highest specific surface areas of all known materials, which is invaluable for applications requiring high levels of surface interactions on a small scale. Of these 2D nanomaterials, nanosilicates are uniquely suited for orthopedic tissue engineering due to their multiple functions such as ability to mechanically reinforce polymeric network, and potential to deliver therapeutic growth factors in a sustained manner.<sup>16–18</sup> Since nanosilicates are composed of complex polyions, they are able to interact within a hydrogel and form strong networks which in turn

increase the mechanical properties.<sup>18–20</sup> In addition to enhanced mechanical properties, the structure of the nanosilicates allow for increased shear-thinning and thixotropic properties when incorporated into polymer solutions.<sup>21, 22</sup> Specifically, nanosilicates independently form noncovalent bonds with multiple polymer strands, which can dynamically break and reform during loading, resulting in shear-thinning and thixotropic gels.<sup>20, 22</sup> The incorporation of these 2D nanoparticles could provide a facile approach in controlling physical and biological properties of the network.

As previously mentioned, most nanocomposite scaffolds for interface tissue are either layered or gradient designs.<sup>3, 4</sup> Layered or stratified scaffolds are the most commonly explored, as these designs often incorporate multiple materials and cell types to mimic the distinct tissue regions.<sup>23</sup> Although the layered scaffolds can account for the different layers of the tissue, i.e. the cartilage and subchondral bone, and possibly the interface region, they are susceptible to delamination because the layers are not necessarily connected. Alternatively, gradient scaffold designs can mimic the gradual change in the physical and mechanical properties that are present at the native tissue interface. In addition, these gradient scaffolds can offer a seamless transition between the two tissue regions and have the potential to mimic the natural structural and mechanical gradients.<sup>5, 24</sup>

Gradient scaffolds have been fabricated using a variety of materials such as hydrogels and nanofibers and fabrication methods including gradient makers, microfluidics, and electrospinning.<sup>25</sup> Electrospun, graded scaffolds have been investigated for the bone-cartilage interface; however, the fibrous structure does not ideally mimic the cartilage region.<sup>26</sup> Alternatively, hydrogel systems have been extensively studied for tissue regeneration due to their tunability and cell microenvironment mimicking capabilities and therefore are also ideal for gradient scaffolds.<sup>27</sup> Specifically for bone and cartilage tissues, previous studies have reported the use of natural material-based hydrogels to support regeneration. For example, gelatin methacryloyl (GelMA) has been investigated for bone regeneration, while methacrylated kappa-carrageenan (MkCA) has been investigated for cartilage regeneration.<sup>9, 18</sup> Although microfluidic methods have been investigated for gradient formation with hydrogels, a simpler approach utilizing capillary flow was previously introduced which allowed for multi-layer gradient hydrogels to be fabricated.<sup>28, 29</sup>

Here, using 2D nanosilicates with two natural polymers, gelatin and kappa carrageenan (kCA), we developed a facile approach to fabricate a nanocomposite gradient hydrogel. Gradient hydrogels were fabricated using the natural material flow properties, which were enhanced by the addition of nanosilicates. A gradient in structure as well as mechanical properties was obtained. In addition, cell morphology was controlled along the scaffold. This simple and reproducible gradient hydrogel fabrication method could be applied to regeneration of tissue interfaces.

## METHODS

### Prepolymer Solution Synthesis

Gelatin (type A, from porcine skin) and methacrylic anhydride (MA) were purchased from Sigma-Aldrich, USA. The synthetic nanosilicates (Laponite-XLG), were obtained from

Southern Clay Product Inc, USA and the kappa-carrageenan was purchased from Tokyo Chemical Industry (TCI), USA. Gelatin methacrylamide (GelMA, 80% methacrylated) and methacrylated kappa-carrageenan (MkCA, 10% methacrylated) were synthesized using previously published methods.<sup>9, 16, 18</sup> Different prepolymer solutions were prepared in deionized water using GelMA (5 % wt/v) and MkCA (1 % wt/v) with varying concentrations of nanosilicates (0, 0.25, 0.5, 0.75 and 1.0 % wt/v). Photoinitiator (IRGACURE 2959, 0.25 % wt/v) was added to the prepolymer solutions. The pre-polymer solutions were prepared via vigorous agitation and heated at 37°C for 15 minutes and were fabricated via UV crosslinking (6.09 mW/cm<sup>2</sup>, 60 seconds).

### Rheology Testing

Rheological properties were characterized for gelation kinetics and shear stress sweeps using DHR-2 Rheometer (TA Instruments). Gelation kinetics of prepolymer solutions under UV irradiation was investigated using a 10 mm parallel plate geometry at a gap of 0.3mm. Oscillatory stress sweeps from 0.1 and 10 Pa at 1 Hz were carried out on all formed hydrogels. The change in viscosity of prepolymer solutions (5% wt/v GelMA and 1% wt/v MkCA, both with and without 0.5% wt/v nanosilicates) were investigated. Samples were pipetted onto a Peltier plate surface and allowed to rest before a 40 mm parallel plate geometry was used to vary the shear rate between 0.01–100 1/s.

### Gradient Hydrogel Fabrication and Optimization

Gradient hydrogels were fabricated using machined Teflon molds (15.50 mm × 6.20 mm), containing three rectangular wells of dimensions 10×2×1 mm. Two different prepolymer solutions of equal volume were pipetted into the either side of the well simultaneously (Figure 1). Upon UV exposure (6.9 mW/cm<sup>2</sup>, 60 secs), the prepolymer solutions were crosslinked to obtain a covalently crosslinked network. Prior to hydrogel formation, the prepolymer solutions were kept in the oven at 37°C. To form uniform gradients, the optimal volume of the prepolymer solutions, as well as the optimal time prior to crosslinking to allow for diffusion were determined. GelMA stained with Rhodamine B and MkCA prepolymers were used and the solutions remained at 37°C until pipetted into the well. For determining the optimal prepolymer volume, three different volumes were tested: 5μL, 10μL, and 15μL. Using the optimal volume, the optimal time prior to crosslinking was tested at 0, 5, and 10 minutes. At time 0, the solutions were added and the mold was immediately exposed to UV. For the other time points, the solutions were added and the mold was placed in the oven at 37°C for 5, or 10 minutes and then exposed to UV. Gradient uniformity was assessed using ImageJ Plot Profile.

### Mechanical Testing

The compressive stress and modulus of the individual hydrogels were tested using MTESTQuattro (ADMENT, USA) with a 25 lb. transducer. The samples were placed in 1X PBS for 1 hour to swell prior to testing. Compression tests were performed and carried out to 50% strain. The compressive modulus was calculated based on the slope of the linear region from the stress-strain curve corresponding to 0–0.2 strain. For gradient hydrogels, compressive tests were performed using a 2 lb. transducer. To test different regions along the gel, an insert with a 1mm cone head was fabricated and prepolymer solutions of varying

compositions were prepared (5% wt/v GelMA and 1% wt/v MkCA with and without nanosilicates). Six locations along the gradient were probed with the 1 mm tip geometry. A MATLAB program was developed to calculate the modulus. Statistical analysis was performed using GraphPad Prism.

### SEM Characterization

To characterize the microstructure and porous nature of the gradient hydrogels, a scanning electron microscope (SEM) was used (JCM-5000: Benchtop SEM (Neoscope)). The gradient hydrogels were fabricated as previously described and then frozen using liquid nitrogen, freeze fractured, and lyophilized overnight. The dried samples were then mounted to expose their cross-section and sputter coated for 60 seconds at 20 mA with gold. The samples were then viewed with the SEM at an accelerating voltage of 10kV. Image analysis was done using ImageJ (NIH).

### In vitro Cell Studies

Human mesenchymal stem cells (hMSCs) were cultured in normal growth media (AMEM, Hyclone), supplemented with 16.5% FBS (Atlanta Biologicals) and 1% penicillin/streptomycin (100U/100 µg/mL; Life Technologies, USA) at 37°C with 5% CO<sub>2</sub>. Prior to cell encapsulation, four Teflon molds were sterilized with 70% ethanol for 15 minutes. Cells were trypsinized, neutralized with normal media, and then spun down at 1000 rpm for 5 minutes. Cell pellets were resuspended in 80µL of the four prepolymer solutions; there were approximately 100,000 cells in each solution. Prepolymer solutions were made in media rather than deionized water and stored at 37°C prior to cell resuspension. Prepolymer solutions containing resuspended cells were then pipetted into the Teflon molds and UV-crosslinked (6.9 mW/cm<sup>2</sup>, 60 seconds). The molds were placed into a 24 well plate with normal media. For cell morphology studies at desired time points, the molds were washed twice with 1X PBS (Corning) and the samples were fixed using 500 µL of 2% glutaraldehyde (Sigma Aldrich) for 20 minutes. Samples were then washed with 1X PBS three times and 500 µL of 0.1% Triton X-100 in 1X PBS was added to permeabilize the cells for 5 minutes. Samples were washed with 1X PBS and gels were removed from Teflon molds for staining. 100 µL of phalloidin (1:100 dilution in 1%BSA/1XPBS) was added and samples were incubated at 37°C and protected from light for 1 hour. After 1 hour, the stain was removed and samples were washed three times with 1X PBS. 100 µL of Propidium Iodine/RNase solution (100 µg/mL RNase and 500 nM-1.5 µM Propidium Iodine) was added, incubated at 37°C for 30 minutes, and then washed three times with 1X PBS. Cell images were taken using a confocal microscope (Leica TCS SP5) and images were analyzed with ImageJ.

### Statistical Analysis

The data are plotted as mean and standard deviation. One-way analysis of variance (ANOVA) with Tukey's post-hoc were performed using Graphpad Prism software. Statistical significance presented as \* p-value<0.05, \*\* p-value< 0.01, \*\*\* p-value<0.001, \*\*\*\*p-value<0.0001.

## RESULTS

Here we have focused on designing a gradient scaffold for interface tissues as the interface contains a gradient in structural, mechanical, and biological properties. Although gradient scaffolds have been investigated previously<sup>2-5</sup>, the presented approach for gradient formation provides a simple and reproducible method that could easily be modified. Previous methods for osteochondral scaffolds have targeted properties such as graded pore size, chemical composition, stiffness, or growth factors.<sup>7, 26, 30, 31</sup> Despite the formation of a gradient to match the gradual change in native tissue, some of these methods can require intensive materials preparation or equipment and only provide a gradual change in one property. In addition, other gradient fabrication methods involve complex microfluidic strategies.<sup>32, 33</sup> The presented method is simple and with two natural polymers and the inclusion of nanosilicates in the hydrogel network, we are able to vary the materials' structural, mechanical, and biological properties.

### Nanoengineered Gradient Hydrogels

Gelatin and  $\kappa$ -carrageenan were ideal polymers for the osteochondral scaffold because of the two have been investigated for bone and cartilage scaffolds individually.<sup>9, 18</sup> Gelatin contains RGD binding domains which allow for cells to adhere and spread typical of osteoblasts in bone; while, kappa carrageenan is a polysaccharide resembling native glycosaminoglycans with limited binding sites, and cells will exhibit a more rounded morphology indicative of chondrocytes in cartilage.<sup>34, 35</sup> In addition, previous studies have demonstrated the mixing capabilities of gelatin and  $\kappa$ -carrageenan in a solution, supporting the mixing of the two solutions in the present gradient hydrogel formation.<sup>36</sup> In the present study, these polymers were successfully modified with methacrylic anhydride to allow for uniform photopolymerization and hydrogel formation. Nanosilicates were incorporated in the two solutions, as previous studies<sup>9, 18</sup> have supported increased shear-thinning and therefore increased flow properties as well as their ability to enhance the structural properties of a material. Specifically for gelatin, as a polyampholytic natural polymer containing both negative and positive regions, it strongly interacts with the opposite charged surfaces of the nanosilicates.<sup>37</sup> In addition, previous gradient constructs, specifically for osteochondral regeneration, have not incorporated nanomaterials into both regions of the scaffold for increased mechanical stability. Finally, human mesenchymal stem cells (hMSCs) were encapsulated within the hydrogel matrix to demonstrate the ability to control cell morphology along the gradient (Figure 1). Here, gradient hydrogels were successfully fabricated using a facile and reproducible method of pipetting two prepolymer solutions into a Teflon mold at the same time and allowing capillary action to form uniform distributions. Although previous studies have demonstrated the ability to form multi-layer gradient hydrogels using capillary flow, here with simple modification, we produced a single but connected layer exhibiting a seamless transition from one material to the next. In addition, the Teflon mold allowed for three hydrogels to be prepared at once for easy replication and the mold fit within a 24-well plate for simple *in vitro* studies.

## Nanosilicate Reinforces Polymeric Network

Prior to gradient hydrogel formation, the optimum concentration of nanosilicates within the 5.0% wt/v GelMA and 1.0% wt/v M $\kappa$ CA hydrogels for improved mechanical properties was determined through compressive mechanical tests (Figure 2). The concentrations of 5.0% wt/v GelMA and 1.0% wt/v M $\kappa$ CA were chosen based on previous studies.<sup>9, 18</sup> The addition of the nanosilicates significantly increased the compressive moduli and strength of the gelatin and  $\kappa$ -carrageenan based hydrogels (Figure 2a & 2b). At 50% compression, the strength of the GelMA hydrogels increased up to seven-fold with the addition of 1% wt/v nanosilicates, while the strength of the M $\kappa$ CA hydrogels increased nearly three-fold at the same concentration. Similarly, with 0.5% wt/v nanosilicates, the strength of GelMA hydrogels increased three-fold while M $\kappa$ CA hydrogels increased two-fold. It was determined that the addition of 0.5% wt/v nanosilicates was the optimal concentration since it provided a significant increase in the M $\kappa$ CA hydrogels' compressive moduli (2.4 $\pm$ 0.3 kPa to 3.4 $\pm$ 0.5 kPa) without increasing the mechanical properties so much that it would mimic the GelMA hydrogels' mechanical properties too closely (Figure 2b). In addition, rather than incorporating another variable to the study, 0.5% wt/v nanosilicates was chosen for the GelMA region as well. Although the addition of 0.5% wt/v nanosilicates was not statistically different from GelMA hydrogels without nanosilicates, the modulus was still increased two-fold (from 3.5 $\pm$ 0.6 kPa to 5.9 $\pm$ 1.8 kPa).

## Nanosilicates Modulate Flow Properties and Rheological Characteristics

With these optimal concentrations, the flow properties of the prepolymer solutions were investigated to evaluate flow once pipetted into the molds. To investigate the effect of nanosilicates on the shear-thinning behavior of prepolymer solutions, the viscosity at different shear rates (0.01–100 1/s) was monitored (Figure 3a). The viscosity decreased with increasing shear rate for all prepolymer compositions suggesting shear-thinning behavior; however, depending on the backbone chemistry and the inclusion of nanosilicates, viscosity can be modulated. Addition of 0.5% wt/v nanosilicates generally causes a solution to have an increase in its shear-thinning ability due to the orientation of the nanoparticle under applied shear.<sup>20, 22</sup> Here, nanosilicates increased the shear-thinning behavior of the prepolymer solutions. Although M $\kappa$ CA nSi was observed to have the highest viscosity, the solution still flowed through the mold.

The gelation kinetics as well as the structural stability of hydrogels at these final concentrations were also investigated (Figure 3b). Methacrylate functional groups on both gelatin and kappa carrageenan permitted covalent crosslinking through UV-initiated free radical polymerization. The addition of nanosilicates did not affect the gelation time of either the GelMA or M $\kappa$ CA hydrogels as indicated by the similar plateaus of the storage modulus; however, the storage modulus was increased by nearly two-fold in the GelMA hydrogels with the addition of the nanosilicates, supporting the increase in mechanical properties seen in compression testing. The rheological data support the results observed in compressive tests, and indicate that only a small percentage of nanosilicates can be incorporated to significantly enhance the mechanical properties of the individual hydrogels.

### Optimizing Gradient Hydrogels

Once the flow properties were determined, the optimal volume to allow each solution to flow towards the middle of the channel as well as the optimal time to allow for uniform distribution of solutions were determined (Figure 4a). Of the three volumes tested, 10  $\mu\text{L}$  of each solution enabled equal flow to the middle. In addition, 5  $\mu\text{L}$  of each solution was too small of a volume to reach the center, while 15  $\mu\text{L}$  nearly overflowed the channel. This even flow was confirmed with the ImageJ Plot Profile in which 10  $\mu\text{L}$  had the most uniform distribution. The Plot Profile tool provided the pixel density along the distance of the gradient; with increasing distance the pixel intensity displayed a sigmoid curve. Using this optimal volume, the ideal time prior to crosslinking was observed to be 5 minutes, which allowed for uniform distribution of both solutions. Although immediate crosslinking after administration allowed for some flow between solutions, quantification with ImageJ revealed a more uniform distribution after 5 minutes (Figure 4b). With these optimal parameters, nanocomposite gradient hydrogels were successfully fabricated.

### Gradient in Structural and Mechanical Properties of Hydrogels

Characterization of the structural and mechanical properties of the gradient hydrogels with and without nanosilicates was performed (Figure 5). The gradient microstructure was observed using SEM and a distinct change in pore area was noted when shifting from the GelMA region ( $4.0 \pm 2.7 \mu\text{m}^2$ ) to the interface region ( $16.9 \pm 14.4 \mu\text{m}^2$ ) and then to the M $\kappa$ CA region ( $75.3 \pm 49.0 \mu\text{m}^2$ ) of the scaffold (Figure 5a). With the addition of nanosilicates, an increase in pore area shifting from the GelMA-nSi region to the M $\kappa$ CA-nSi region was also observed (Figure 5b). Previous studies have reported an increase in pore size in GelMA hydrogels due to interactions of the nanosilicates with the gelatin backbone, supporting the increase observed in this study.<sup>18</sup> Alternatively, pore size was previously observed to decrease with the addition of nanosilicates in M $\kappa$ CA hydrogels.<sup>9</sup> This discrepancy could result from changes in M $\kappa$ CA and nanosilicate concentrations; the concentrations used in this study are smaller than those used in the previous study and therefore could affect the way the materials interact together. At the interface regions, a range of pore sizes exists which leads to high standard deviations but demonstrates the integration of the two natural polymers.

To characterize the mechanical properties of gradient structures, compression tests were performed using a 1mm cone geometry that allowed for different regions along the scaffold to be probed (Figure 5a & 5b). For all hydrogels, a total of six regions along the gel were tested. For both gradients, a decrease in the compression modulus was observed when shifting from the GelMA regions to the M $\kappa$ CA regions, supporting previously observed compressive moduli values for individual hydrogels. Specifically in the hydrogels without nanosilicates, the moduli shifted from  $6.7 \pm 0.4 \text{ kPa}$  in the GelMA region to  $1.8 \pm 0.4 \text{ kPa}$  in the M $\kappa$ CA region. When nanosilicates were incorporated, the moduli decreased from  $7.5 \pm 1.7 \text{ kPa}$  in the GelMA nSi region to  $3.6 \pm 1.8 \text{ kPa}$  in the M $\kappa$ CA nSi region. Prior to performing compression tests on the gradient scaffolds, the new 1mm cone geometry was validated by testing GelMA hydrogels and resulting moduli values were compared to published results.<sup>18</sup>



## hMSC Encapsulation Exhibits Gradient in Cell Morphology

The cellular response at different regions of the gradient hydrogels was investigated through 3D encapsulation of human mesenchymal stem cells (hMSCs) (Figure 6a). hMSCs were successfully encapsulated within the hydrogel networks and imaged after one and three days. After one day, cells remained round in all regions of both gradient scaffolds. However, after three days of encapsulation, a distinct change in cell morphology was observed based on the location within the gradient. In the GelMA and GelMA-nSi regions, cells were spread out characteristic of osteoblasts in bone, while the MκCA and MκCA-nSi regions, cells exhibited a round morphology characteristic of chondrocytes in cartilage.<sup>38</sup> At the interface regions, both cell morphologies were present, indicating a smooth transition from one region to the next (Figure 6b). These results reinforce previous studies that suggest GelMA and MκCA to support bone and cartilage regeneration respectively.<sup>9, 18</sup>

Average cell circularity and cell area along the scaffold were calculated using ImageJ to quantify these changes in cell morphology (Figure 6c & 6d). Circularity (a.u) ranged from 0–1, in which 1 represented a perfect circle. In the GelMA region, the average cell circularity was found to be  $0.4 \pm 0.2$  while in the MκCA region this increased significantly to  $0.8 \pm 0.1$ . At the interface, the average cell circularity was  $0.5 \pm 0.3$ , in between the average for the two extreme regions of the scaffold. With the addition of nanosilicates, the average cell circularity was not significantly affected; however, a similar trend in cell circularity was observed from the GelMA nSi region to the MκCA nSi region.

In addition to circularity, the average cell area along the gradient scaffolds was calculated. Average cell area decreased from the GelMA region ( $783.5 \pm 354.7 \mu\text{m}^2$ ) where cells were spread out, to the interface region ( $656.9 \pm 300.1 \mu\text{m}^2$ ) and to the MκCA region ( $431.3 \pm 169.5 \mu\text{m}^2$ ) where cells were more rounded (Figure 6c). When nanosilicates were incorporated into the scaffold, average cell area was not significantly affected but a similar trend existed.

## DISCUSSION

Gradient scaffolds were successfully fabricated utilizing gelatin, κ-carrageenan, and nanosilicates in a facile microfabrication process. Previously, gelatin and κ-carrageenan have shown to mix well in solution, supporting the ability to form a gradient.<sup>36, 39</sup> In addition, once in solution together, the polymers interact with one another via electrostatic interactions.<sup>39</sup> These initial interactions may allow for the solutions to be loosely bound prior to UV crosslinking and further enhance the connectivity of the scaffold. Additionally, incorporation of nanosilicates with these two natural materials have previously shown to enhance shear-thinning characteristics as well as structural and mechanical properties via electrostatic interactions.<sup>9, 18</sup> Structural, mechanical, and biological gradients were successfully generated in the micro-fabricated scaffolds utilizing these natural polymers and nanosilicates.

Investigating the gradient hydrogels' microstructures via SEM revealed a gradient in the structure, specifically with the changes in pore size. Pore size is important for nutrient diffusion as well as cell infiltration in the scaffold.<sup>40</sup> For bone regeneration, some studies

have reported optimal pore sizes around 100  $\mu\text{m}$ , while others have suggested lower pore size around 16  $\mu\text{m}$  to support osteogenesis.<sup>41, 42</sup> In the present study, the pore size of the GelMA regions of the scaffold fall within this smaller range; however, previous studies investigating GelMA for bone regeneration have demonstrated this pore size to be sufficient.<sup>18</sup> Similarly for cartilage regeneration, a previous study suggested pore size within the range of 50 to 500  $\mu\text{m}$  to support chondrogenesis and as the pore size increased, cartilage specific markers increased.<sup>43</sup> Here, the pore size of M $\kappa$ CA fell within this range. Overall, the observed increase in pore area across the hydrogels indicated the formation of a structural gradient in the two scaffolds. This gradient in pore size could promote cell differentiation along the scaffold for bone-cartilage regeneration.

In addition, a gradient in mechanical properties was observed across the scaffold via compression tests. Although a gradual change in moduli was observed, high error was still present in some of the samples as a result of the small sample and sample geometry. In addition, achieving reproducibility in the six regions tested along the gradient hydrogel was difficult. Regardless of these difficulties, a distinct transition in the mechanical properties of both gradient hydrogels was observed indicating successful fabrication of a gradient in mechanical properties. As previously discussed, hydrogel stiffness can be influential in directing cell morphology and possibly cell differentiation.<sup>44, 45</sup> With the present gradient in the nanocomposite's mechanical properties, the scaffold holds the potential to further stimulate cell morphology and subsequently cell differentiation along the different regions.

Finally, encapsulated hMSCs demonstrated a gradient in the biological properties of the scaffold, specifically through observation of changes in cell morphology along the gradient. Although the standard deviation in average cell area was high in the GelMA and interface regions with and without nanosilicates, this is most likely a result of the projection of images required to obtain a clean image with encapsulated cells which then layered cells over one another making it difficult to distinguish individual cells. In addition, although the majority of the GelMA and GelMA-nSi regions contained cells exhibiting spread morphologies, some round cells were still present, bringing down the average area and increasing the standard deviation. Unfortunately, the role of nanosilicates in directing cell morphology was not as pronounced at the low chosen concentration even though the addition significantly affected mechanical properties of the scaffold. These cell encapsulation studies indicated the ability to control cell morphology along a gradient scaffold. Although cell differentiation was not investigated in this study, this change in cell shape along the nanocomposite implies the potential for controlling cell fate. More importantly, cell morphology was controlled with just the material selection and incorporation of nanosilicates. This fabrication platform can be used to generate 3D microarrays to rapidly interrogate cell-matrix interactions.<sup>46</sup>

Overall, in this study we have introduced a simple and reproducible approach for fabricating nanocomposite gradient hydrogels. The inclusion of nanosilicates, a novel 2D nanomaterial, allowed for control over the structural, mechanical, and biological properties. Specifically, the structural and mechanical properties of the gradient hydrogel were characterized demonstrating the ability to vary these properties through material selection and generate a gradient in these physical properties. In addition, successful cell encapsulation and control over cell morphology demonstrates the potential to direct cell fate within the network and

possibly direct cell differentiation without the use of growth factors. This simple approach could be applied to regeneration of the bone-cartilage interface where a natural gradient in the structural, mechanical, and biological properties exists as well as tailored to other tissue engineering applications.

## Acknowledgments

LC would like to acknowledge financial support from Texas A&M University Diversity Fellowship. AKG would like to acknowledge funding support from Texas Engineering Experiment Station and Texas A&M University Seed Grant.

## References

1. Hoemann CD, Lafantaisie-Favreau CH, Lascau-Coman V, Chen G, Guzman-Morales J. The cartilage-bone interface. *The journal of knee surgery*. 2012; 25:85–97. [PubMed: 22928426]
2. Nukavarapu SP, Dorcenus DL. Osteochondral tissue engineering: Current strategies and challenges. *Biotechnology Advances*. 2013; 31:706–721. [PubMed: 23174560]
3. Sant S, Hancock MJ, Donnelly JP, Iyer D, Khademhosseini A. Biomimetic gradient hydrogels for tissue engineering. *The Canadian journal of chemical engineering*. 2010; 88:899–911. [PubMed: 21874065]
4. Singh M, Berklund C, Detamore MS. Strategies and applications for incorporating physical and chemical signal gradients in tissue engineering. *Tissue Engineering Part B: Reviews*. 2008; 14:341–366. [PubMed: 18803499]
5. Cross LM, Thakur A, Jalili NA, Detamore M, Gaharwar AK. Nanoengineered biomaterials for repair and regeneration of orthopedic tissue interfaces. *Acta Biomaterialia*. 2016; 42:2–17. [PubMed: 27326917]
6. Khanarian NT, Haney NM, Burga RA, Lu HH. A functional agarose-hydroxyapatite scaffold for osteochondral interface regeneration. *Biomaterials*. 2012; 33:5247–5258. [PubMed: 22531222]
7. Liu C, Han Z, Czernuszka JT. Gradient collagen/nanohydroxyapatite composite scaffold: Development and characterization. *Acta Biomaterialia*. 2009; 5:661–669. [PubMed: 18990616]
8. Xue D, Zheng Q, Zong C, Li Q, Li H, Qian S, et al. Osteochondral repair using porous poly(lactide-co-glycolide)/nano-hydroxyapatite hybrid scaffolds with undifferentiated mesenchymal stem cells in a rat model. *Journal of Biomedical Materials Research Part A*. 2010; 94A:259–270.
9. Thakur A, Jaiswal MK, Peak CW, Carrow JK, Gentry J, Dolatshahi-Pirouz A, et al. Injectable shear-thinning nanoengineered hydrogels for stem cell delivery. *Nanoscale*. 2016; 8:12362–12372. [PubMed: 27270567]
10. Carrow JK, Gaharwar AK. Bioinspired Polymeric Nanocomposites for Regenerative Medicine. *Macromolecular Chemistry and Physics*. 2015; 216:248–264.
11. Jalili NA, Muscarello M, Gaharwar AK. Nanoengineered Thermoresponsive Magnetic Hydrogels for Biomedical Applications. *Bioengineering & Translational Medicine*. 2016; 1:297–305. [PubMed: 29313018]
12. Parani M, Lokhande G, Singh A, Gaharwar AK. Engineered Nanomaterials for Infection Control and Healing Acute and Chronic Wounds. *ACS Applied Materials & Interfaces*. 2016; 8:10049–10069. [PubMed: 27043006]
13. Gaharwar AK, Peppas NA, Khademhosseini A. Nanocomposite hydrogels for biomedical applications. *Biotechnology and Bioengineering*. 2014; 111:441–453. [PubMed: 24264728]
14. Chimene D, Alge DL, Gaharwar AK. Two-Dimensional Nanomaterials for Biomedical Applications: Emerging Trends and Future Prospects. *Advanced Materials*. 2015; 27:7261–7284. [PubMed: 26459239]
15. Kerativitayanan P, Carrow JK, Gaharwar AK. Nanomaterials for Engineering Stem Cell Responses. *Advanced Healthcare Materials*. 2015; 4:1600–1627. [PubMed: 26010739]

16. Mihaila SM, Gaharwar AK, Reis RL, Marques AP, Gomes ME, Khademhosseini A. Photocrosslinkable kappa-carrageenan hydrogels for tissue engineering applications. *Advanced healthcare materials*. 2013; 2:895–907. [PubMed: 23281344]
17. Mihaila SM, Gaharwar AK, Reis RL, Khademhosseini A, Marques AP, Gomes ME. The osteogenic differentiation of SSEA-4 sub-population of human adipose derived stem cells using silicate nanoplatelets. *Biomaterials*. 2014; 35:9087–9099. [PubMed: 25123923]
18. Xavier JR, Thakur T, Desai P, Jaiswal MK, Sears N, Cosgriff-Hernandez E, et al. Bioactive Nanoengineered Hydrogels for Bone Tissue Engineering: A Growth-Factor-Free Approach. *ACS Nano*. 2015; 9:3109–3118. [PubMed: 25674809]
19. Gaharwar AK, Rivera CP, Wu CJ, Schmidt G. Transparent, elastomeric and tough hydrogels from poly(ethylene glycol) and silicate nanoparticles. *Acta Biomaterialia*. 2011; 7:4139–4148. [PubMed: 21839864]
20. Ruzicka B, Zaccarelli E. A fresh look at the Laponite phase diagram. *Soft Matter*. 2011; 7:1268–1286.
21. Peak CW, Carrow JK, Thakur A, Singh A, Gaharwar AK. Elastomeric Cell-Laden Nanocomposite Microfibers for Engineering Complex Tissues. *Cell Mol Bioeng*. 2015; 8:404–415.
22. Gaharwar AK, Avery RK, Assmann A, Paul A, McKinley GH, Khademhosseini A, et al. Shear-Thinning Nanocomposite Hydrogels for the Treatment of Hemorrhage. *ACS Nano*. 2014; 8:9833–9842. [PubMed: 25221894]
23. Liverani L, Roether JA, Noeaid P, Trombetta M, Schubert DW, Boccaccini AR. Simple fabrication technique for multilayered stratified composite scaffolds suitable for interface tissue engineering. *Materials Science and Engineering: A*. 2012; 557:54–58.
24. Lu HH, Thomopoulos S. Functional Attachment of Soft Tissues to Bone: Development, Healing, and Tissue Engineering. *Annual review of biomedical engineering*. 2013; 15:201–226.
25. Seidi A, Ramalingam M, Elloumi-Hannachi I, Ostrovidov S, Khademhosseini A. Gradient biomaterials for soft-to-hard interface tissue engineering. *Acta Biomaterialia*. 2011; 7:1441–1451. [PubMed: 21232635]
26. Eriskin C, Kalyon DM, Wang H. Functionally graded electrospun polycaprolactone and  $\beta$ -tricalcium phosphate nanocomposites for tissue engineering applications. *Biomaterials*. 2008; 29:4065–4073. [PubMed: 18649939]
27. Slaughter BV, Khurshid SS, Fisher OZ, Khademhosseini A, Peppas NA. Hydrogels in Regenerative Medicine. *Advanced Materials*. 2009; 21:3307–3329. [PubMed: 20882499]
28. Hancock MJ, He JK, Mano JF, Khademhosseini A. Surface-Tension-Driven Gradient Generation in a Fluid Stripe for Bench-Top and Microwell Applications. *Small*. 2011; 7:892–901. [PubMed: 21374805]
29. Piraino F, Camci-Unal G, Hancock MJ, Rasponi M, Khademhosseini A. Multi-gradient hydrogels produced layer by layer with capillary flow and crosslinking in open microchannels. *Lab Chip*. 2012; 12:659–661. [PubMed: 22167009]
30. Tang G, Zhang H, Zhao Y, Zhang Y, Li X, Yuan X. Preparation of PLGA scaffolds with graded pores by using a gelatin-microsphere template as porogen. *Journal of biomaterials science Polymer edition*. 2012; 23:2241–57. [PubMed: 22137329]
31. Mohan N, Dormer NH, Caldwell KL, Key VH, Berkland CJ, Detamore MS. Continuous gradients of material composition and growth factors for effective regeneration of the osteochondral interface. *Tissue engineering Part A*. 2011; 17:2845–55. [PubMed: 21815822]
32. Pedron S, Peinado C, Bosch P, Benton JA, Anseth KS. Microfluidic approaches for the fabrication of gradient crosslinked networks based on poly(ethylene glycol) and hyperbranched polymers for manipulation of cell interactions. *Journal of Biomedical Materials Research Part A*. 2011; 96A:196–203.
33. Mahadik BP, Wheeler TD, Skertich LJ, Kenis PJA, Harley BAC. Microfluidic Generation of Gradient Hydrogels to Modulate Hematopoietic Stem Cell Culture Environment. *Advanced healthcare materials*. 2014; 3:449–458. [PubMed: 23997020]
34. Campo VL, Kawano DF, Silva DBd Jr, Carvalho I. Carrageenans: Biological properties, chemical modifications and structural analysis – A review. *Carbohydrate Polymers*. 2009; 77:167–180.

35. Nichol JW, Koshy ST, Bae H, Hwang CM, Yamanlar S, Khademhosseini A. Cell-laden microengineered gelatin methacrylate hydrogels. *Biomaterials*. 2010; 31:5536–5544. [PubMed: 20417964]
36. Fang Y, Li L, Inoue C, Lundin L, Appelqvist I. Associative and Segregative Phase Separations of Gelatin/ $\kappa$ -Carrageenan Aqueous Mixtures. *Langmuir*. 2006; 22:9532–9537. [PubMed: 17073476]
37. Pawar N, Bohidar HB. Surface selective binding of nanoclay particles to polyampholyte protein chains. *The Journal of Chemical Physics*. 2009; 131:045103. [PubMed: 19655924]
38. Fuß M, Ehlers EM, Russlies M, Rohwedel J, Behrens P. Characteristics of human chondrocytes, osteoblasts and fibroblasts seeded onto a type I/III collagen sponge under different culture conditions. *Annals of Anatomy - Anatomischer Anzeiger*. 2000; 182:303–310. [PubMed: 10932320]
39. Antonov YA, Gonçalves MP. Phase separation in aqueous gelatin– $\kappa$ -carrageenan systems. *Food Hydrocolloids*. 1999; 13:517–524.
40. Annabi N, Nichol JW, Zhong X, Ji C, Koshy S, Khademhosseini A, et al. Controlling the Porosity and Microarchitecture of Hydrogels for Tissue Engineering. *Tissue Engineering Part B: Reviews*. 2010; 16:371–383. [PubMed: 20121414]
41. Kim HJ, Kim UJ, Vunjak-Novakovic G, Min BH, Kaplan DL. Influence of macroporous protein scaffolds on bone tissue engineering from bone marrow stem cells. *Biomaterials*. 2005; 26:4442–4452. [PubMed: 15701373]
42. Whang K, Healy KE, Elenz DR, Nam EK, Tsai DC, Thomas CH, et al. Engineering bone regeneration with bioabsorbable scaffolds with novel microarchitecture. *Tissue Eng*. 1999; 5:35–51. [PubMed: 10207188]
43. Lien SM, Ko LY, Huang TJ. Effect of pore size on ECM secretion and cell growth in gelatin scaffold for articular cartilage tissue engineering. *Acta Biomaterialia*. 2009; 5:670–679. [PubMed: 18951858]
44. Subramony S, Dargis B, Castillo M, Azeloglu E, Tracey M, Su A, et al. The guidance of stem cell differentiation by substrate alignment and mechanical stimulation. *Biomaterials*. 2013; 34:1942–1953. [PubMed: 23245926]
45. Tse JR, Engler AJ. Stiffness Gradients Mimicking In Vivo Tissue Variation Regulate Mesenchymal Stem Cell Fate. *PLoS ONE*. 2011; 6:e15978. [PubMed: 21246050]
46. Gaharwar AK, Arpanaei A, Andresen TL, Dolatshahi-Pirouz A. 3D Biomaterial Microarrays for Regenerative Medicine: Current State-of-the-Art, Emerging Directions and Future Trends. *Advanced Materials*. 2016; 28:771–781. [PubMed: 26607415]

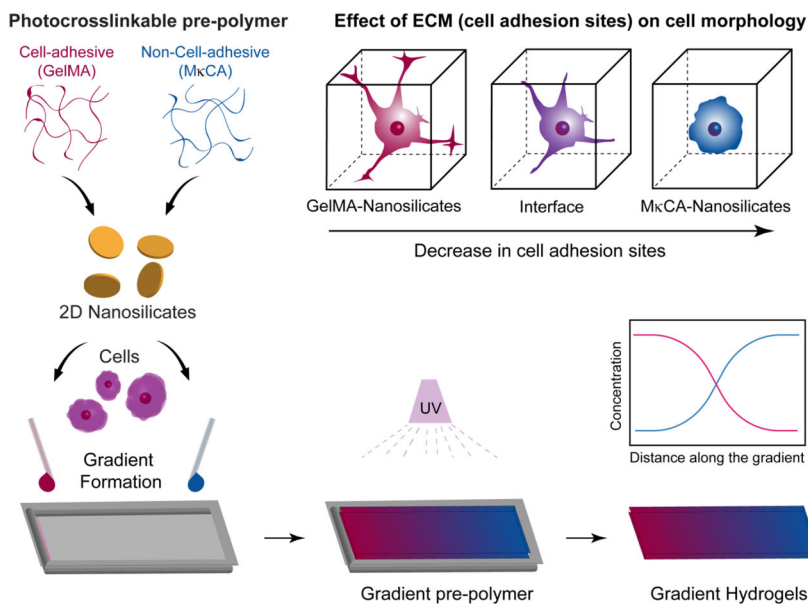


**Fig. 1. Nanoengineered gradient scaffolds loaded with 2D nanoparticles**  
 Schematic showing formation of gradient hydrogel from GelMA and MκCA prepolymers reinforced with nanosilicates (nSi). Cells can be encapsulated during the formation of gradient scaffold. The gradient structure is subjected to UV light to obtain fully crosslinked scaffold. The GelMA contains cell binding sites which allow for cell spreading, whereas the MκCA does not and cells are expected to retain a round morphology.

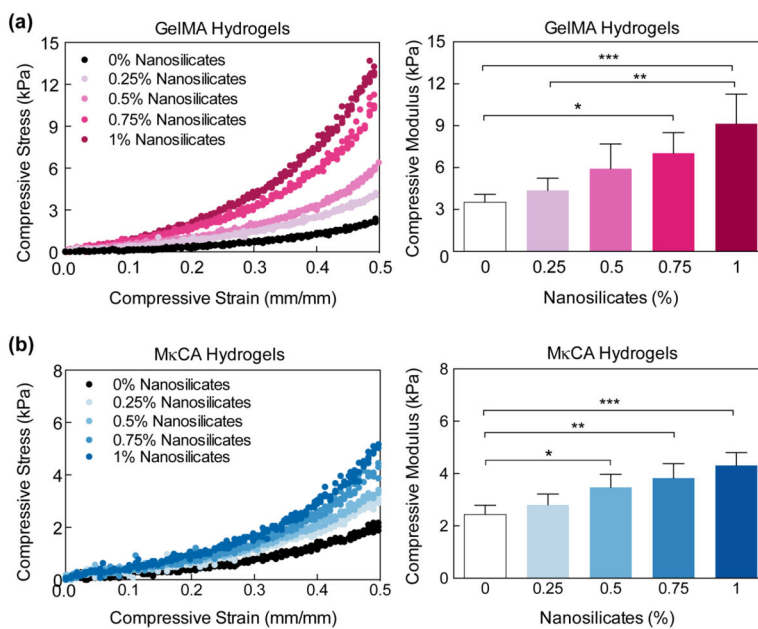


**Fig. 2. Nanosilicates reinforce the polymeric hydrogels**

(a) Uniaxial compression test show that addition of nanosilicates to (a) GelMA and (b) MκCA hydrogel results in an increase in compressive modulus. (Statistical Analysis: One-way Anova with Tukey’s post-hoc analysis, \* p-value<0.05, \*\* p-value< 0.01, \*\*\* p-value<0.001).

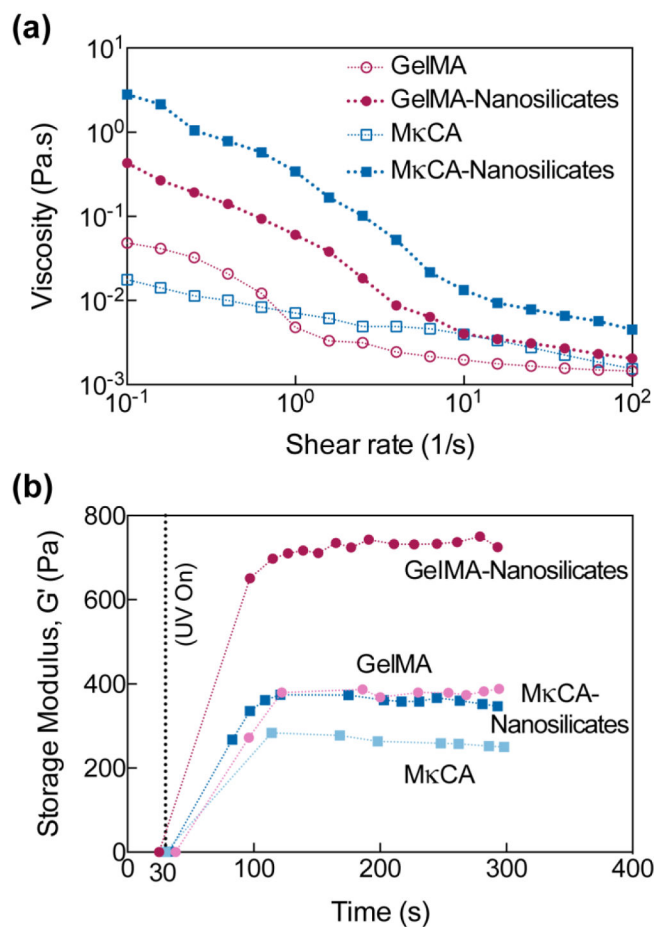


**Fig. 3. Nanosilicates modulate flow and rheological properties of prepolymer solution**

(a) The addition of 0.5% wt/v nSi allowed the GelMA and MκCA prepolymer solutions to exhibit shear-thinning behavior, a decrease in viscosity with increasing shear rate. (b) UV gelation kinetics reveal an increase in storage modulus but no increase in gelation time with incorporation of 0.5% wt/v nSi in either GelMA or MκCA.



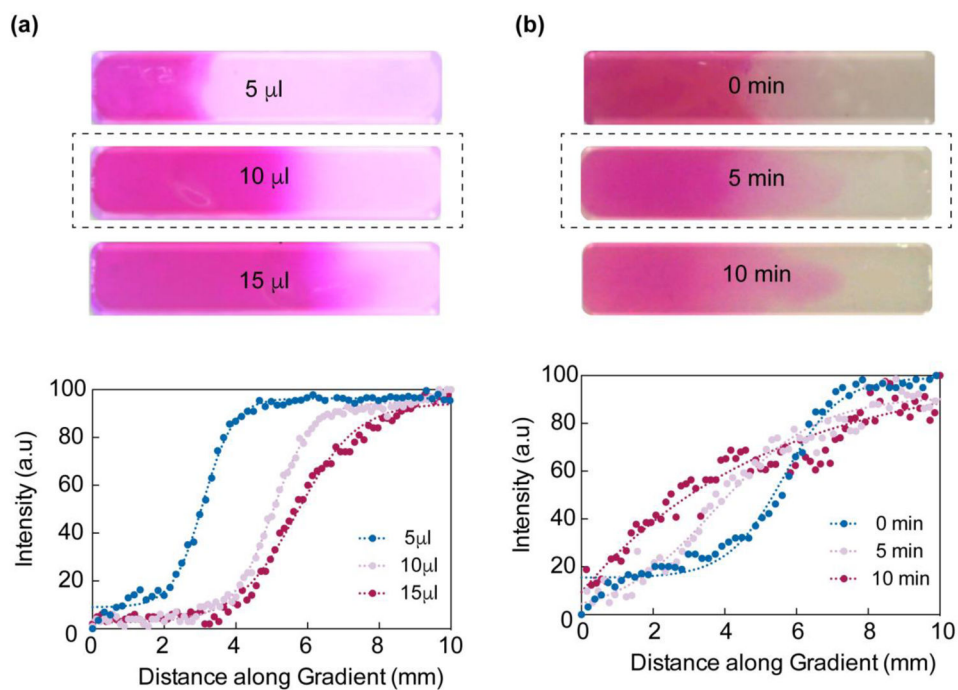


**Fig. 4. Fabrication of gradient hydrogels**

(a) Optimization of solution volume to form uniform gradients revealed 10  $\mu\text{L}$  of each solution allowed for immediate mixing (top). ImageJ quantification supported this observation (bottom). (b) Optimal time for uniform mixing of solutions once pipetted was observed to be 5 minutes (top). Similarly, quantification in ImageJ revealed the most uniform curve (bottom).

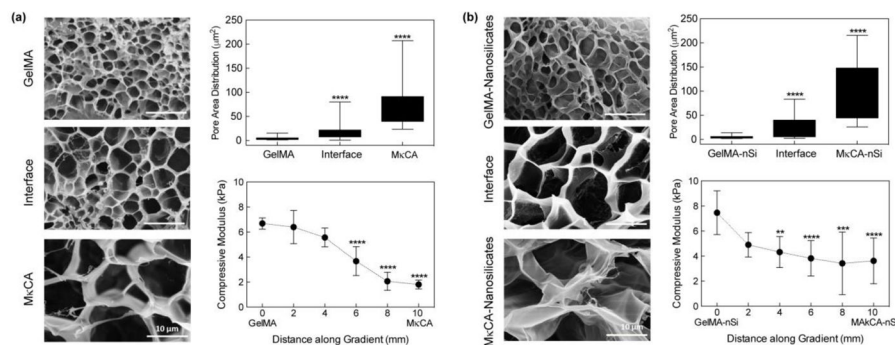


**Fig. 5. Gradient in microstructure and mechanical stiffness of scaffold**

(a) Scanning electron micrographs of gradient hydrogels (GelMA- MκCA). A significant increase in pore size was observed at the interface and MκCA regions, compared to the GelMA region. Compression testing of gradient hydrogels revealed a gradual decrease in compressive moduli when shifting from GelMA region to MκCA region. (b) The addition of nanosilicates (nSi) increased the overall gradient hydrogel pore size with a significant increase in the interface and MκCA nSi regions compared to the GelMA nSi region. Similarly, mechanical testing revealed a gradual decrease in compressive moduli but the inclusion of nSi increased the overall compressive moduli two-fold. (Statistical Analysis: One-way Anova with Tukey’s post-hoc analysis, \* p-value<0.05, \*\* p-value< 0.01, \*\*\* p-value<0.001, \*\*\*\*p-value<0.0001)

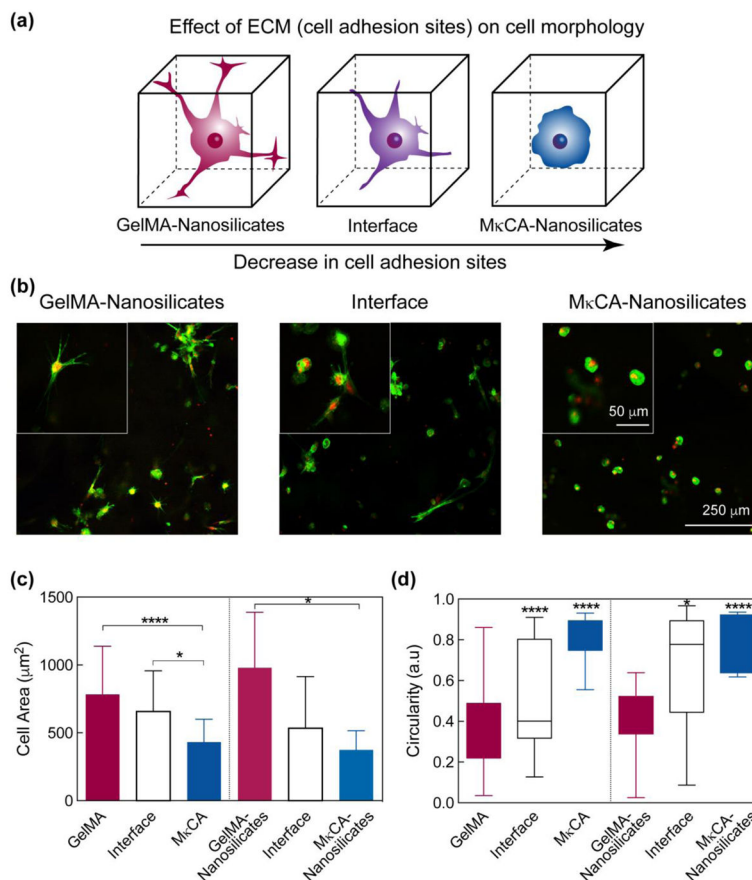


**Fig. 6. Gradient in cell adhesion and morphology**

(a) Schematic demonstrating change in cell morphology along gradient hydrogel. As the cell adhesion sites decrease, the cell morphology becomes more round. (b) Increased cell spreading was observed in the GelMA nSi region after three days of culture while in the MκCA nSi region, cell morphology remained significantly round. At the interface region, both cell morphologies were present. (c) Cell area decreased along the gradient scaffold from the GelMA to MκCA region. The addition of nanosilicates increased the cell area in the GelMA region while its inclusion did not significantly affect the cell area in the MκCA or interface regions. (d) Similarly, cell circularity was much greater in the MκCA regions compared to the GelMA regions where cells were observed to be more spread out. (Statistical Analysis: One-way Anova with Tukey’s post-hoc analysis, \* p-value<0.05, \*\* p-value< 0.01, \*\*\* p-value<0.001, \*\*\*\*p-value<0.0001)